Journal of Sound and Vibration (2000) **238**(2), 189–214
doi:10.1006/jsvi.2000.3082, available online at http://www.idealibrary.com on IDEAL®

A HYBRID PSEUDO-FORCE/LAPLACE TRANSFORM METHOD FOR NON-LINEAR TRANSIENT RESPONSE OF A SUSPENDED CABLE

Y. Q. Ni

Department of Civil and Structural Engineering, The Hong Kong Polytechnic University, Kowloon, Hong Kong. E-mail: ceyqni@polyu.edu.hk

W. J. Lou

Department of Civil and Structural Engineering, The Hong Kong Polytechnic University, Kowloon, Hong Kong
Department of Civil Engineering, Zhejiang University, Hangzhou 310027, *People's Republic of China*

AND

J. M. Ko

Department of Civil and Structural Engineering, The Hong Kong Polytechnic University, Kowloon, Hong Kong. E-mail: cejmko@polyu.edu.hk

(*Received* 26 *November* 1999, *and in final form* 3 *May* 2000)

A hybrid numerical scheme involving the combination of the Laplace transform technique and the pseudo-force method is proposed to analyze the non-linear transient response of a suspended cable subjected to arbitrary dynamic loading. A theoretical model of the cable with multi-degree-of-freedom is first obtained through discretization of the partial differential equations by finite difference approximation. The non-linear governing equations take into account the effects of quadratic and cubic geometric non-linearities. The proposed method deals with the non-linear effects as pseudo-forces and then establishes an iterative solution scheme in the alternating Laplace/time domain by means of fast numerical Laplace transform. This method eschews a time-stepping process and therefore is computationally efficient. It also readily deals with the viscoelastic damping with frequency-dependent model parameters and the hysteresis damping in terms of complex stiffness models. Numerical examples are presented to evaluate the dynamic responses of suspended cables under a concentrated sinusoidal force and a distributed random excitation, and to identify the non-linear response properties by comparison with the linear vibration. The validity and accuracy of the proposed method is also verified by comparing the results with those obtained by using the direct time integration.

1. INTRODUCTION

The suspended cable has a wide range of practical applications in civil engineering and in electrical industry. Long-span suspension bridges have become increasingly popular in recent years due to their effective use of materials and their pleasant aesthetics. The noteworthy records are the Tsing Ma Bridge of 1377 m, the Jiangyin Bridge of 1385 m, the Humber Bridge of 1410 m, the Great Belt East Bridge of 1624 m, and the Akashi-Kaikyo Bridge of 1991 m which is the world's longest suspension bridge at present. The aerodynamics of the free cable-tower system is an important engineering issue in

0022-460X/00/470189 + 26 $35.00/0

wind-resistant design of suspension bridges because the maximum danger of flutter-type aerodynamics instability occurs during the early erection stage of the main cables suspended with a few partially erected deck units [1, 2]. The dynamic response analysis of free main cables of suspension bridges under synchronous and non-synchronous seismic support-excitations is another research topic of practical interest [3, 4]. The research interest in this aspect has been recently enhanced due to the attack of the 1995 Kobe Earthquake on the erected Akashi-Kaikyo Bridge. At the time of this earthquake, both the towers and main cables of the bridge were erected but no deck units had been hoisted [5]. For the suspended cables with long span and large sag, the effect of geometric non-linearity on the dynamic response is significant, especially when subjected to strong wind and earthquake excitations.

The prominent linear theory developed by Irvine and Caughey [6] describes the in-plane and out-of-plane free vibration of a suspended cable with small sag and two fixed supports at the same level. Hagedorn and Schafer [7] were among the first to extend the linear theory to account for geometric non-linearities of the cable. Subsequently, numerous investigations have been made to study different aspects of non-linear free and periodic/quasi-periodic vibrations of suspended cables [8–17], especially the external and internal resonances. In these studies, a discretized model with a few (two to four) degrees of freedom (d.o.f.) was first derived by applying the Galerkin procedure to the governing partial differential equations making use of the linearized modal deflection functions, and then the method of multiple scales or other perturbation techniques were adopted to obtain the response prediction. However, a study by Pakdemirli *et al.* [18] showed that treatment of the discretized system in modal co-ordinates might result in inaccurate results compared to direct treatment of the partial differential equations in some circumstances. Much less research has been devoted to the transient dynamics of geometrically non-linear cables. At present, the time-step integration procedure applied to the discretized finite element or finite-difference model seems to be the only way to obtain the non-linear transient dynamic responses of cables. For example, Wu and Chen [19] studied the moving-load-induced vibrations of a suspended cable by using the Newmark direct integration method incorporated with the Newton–Raphson iteration technique; Wang *et al.* [20] combined the finite element method and the Runge–Kutta method to analyze underwater vibrations of a cable; Koh *et al.* [21] used a modified box scheme (finite difference approximation in both space and time domains) in conjunction with a time-step iterative method for the dynamic analysis of low-tension cables.

When the direct integration approach in the time domain is used to solve for non-linear transient problems, it is often necessary to take very small time steps to avoid undesirable numerical oscillations (high-frequency oscillations) in the solution process. It will cost a great deal of computational effort to obtain a long-term solution, especially for a system with many d.o.f. The pseudo-force method [22, 23] and the incremental mode superposition technique [24, 25] have also been used for non-linear response analysis, but both of them are still step-by-step time-marching scheme. The hybrid frequency–time domain (HFTD) method developed for soil–structure interaction analysis [26, 27] has been shown to be an efficient numerical procedure in solving non-linear transient responses. In this method an alternating frequency/time-domain iterative scheme based on the fast Fourier transform (FFT) is adopted instead of the time-marching process. It has also been noted that a combined Laplace transform and increment linearization approach [28] was successfully applied to the evaluation of non-linear foundation uplifting under earthquake loads. However, this method is only applicable to piecewise linear systems.

In the present study, a hybrid pseudo-force/Laplace transform method is presented for non-linear transient response analysis of suspended cables under arbitrary dynamic

loading. A multi d.o.f. model is first formulated by discretizing the governing partial differential equations of motion in finite-difference form. The proposed method then treats the non-linear terms of quadratic and cubic non-linearities as pseudo-forces. With the response time history of the linearized system as initial guesses, the pseudo-forces are estimated for all values of time and the linearized ordinary differential equations are solved by numerically transforming to the Laplace domain. The displacement responses in the time domain are then obtained by numerical inversion of the Laplace solution and the pseudo-forces are updated. The process is repeated iteratively until convergence is reached. The segmenting approach [26] is introduced in the solution scheme to ensure the convergence. Compared with the HFTD method, the proposed method possesses two advantages. Firstly, the present method allows the incorporation of initial conditions, and therefore gives rise to more accurate transient response prediction than the HFTD method. Secondly, due to the imposed periodicity of the discretized functions in FFT and the resulting convolution error, a decaying loading function as the appended function at the end of the time segment is necessary for the HFTD method [27]. In contrast, the present method does not suffer from this deficiency and therefore the algorithm is more efficient.

2. SYSTEM DESCRIPTION

2.1. EQUATIONS OF MOTION

As shown in Figure 1, a heavy elastic cable suspended between two fixed supports at the same level is considered. The cable has shallow sag with the sag-to-span ratio ranging from nearly zero to about 1:8. Let L, E, A, and m be the cable length, the modulus of elasticity, the cross-sectional area and the mass per unit length of cable, respectively, l be the span. The cable tension in the static configuration is $T = T(s)$. The static equilibrium configuration lies in a vertical plane x–y and is described by a known function $y(s)$, s being a curvilinear abscissa. The dynamic configuration subjected to vertical distributed dynamic loading $f(s, t)$ is described by the displacement components $u(s, t)$ and $v(s, t)$ measured from the static equilibrium position in the longitudinal and vertical directions respectively.

It is assumed that the initial static strain is negligible with respect to unity. With the Lagrangian strain as strain measure, the cable extensional strain due to dynamic loads can be expressed by retaining terms up to order v^3 as [16]

$$\varepsilon = \frac{\partial u}{\partial x} + \frac{\mathrm{d}y}{\mathrm{d}x}\frac{\partial v}{\partial x} + \frac{1}{2}\left(\frac{\partial v}{\partial x}\right)^2. \tag{1}$$

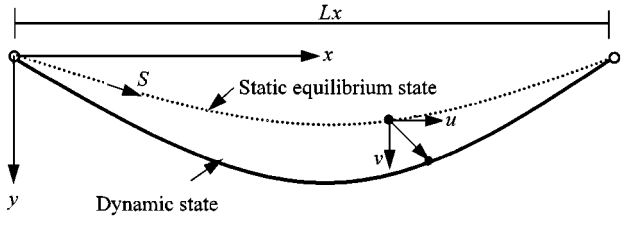

Figure 1. Cable configurations.

The governing differential equations of planar motion of a suspended cable can be derived using the Hamilton principle

$$\delta H = \delta \int_{t_1}^{t_2} \int_0^L (Q - V)\,\mathrm{d}s\,\mathrm{d}t + \int_{t_1}^{t_2} \int_0^L \delta W\,\mathrm{d}s\,\mathrm{d}t = 0 \tag{2}$$

in which Q is the kinetic energy density, V the elastic strain energy density, δW the virtual work density associated with the gravity, dynamic loading and damping force. They are expressed as

$$Q = \frac{m}{2}\left[\left(\frac{\partial u}{\partial t}\right)^2 + \left(\frac{\partial v}{\partial t}\right)^2\right], \quad V = V_i + \frac{EA}{2}\varepsilon^2 + T\varepsilon, \tag{3a,b}$$

$$\delta W = \left[mg + f(s,t) - c_y\frac{\partial v}{\partial t}\right]\delta v - c_x\frac{\partial u}{\partial t}\,\delta u, \tag{3c}$$

where V_i is the elastic strain energy density held in the initial (static) configuration, c_x and c_y are the viscous damping coefficients per unit length in the longitudinal and vertical directions respectively.

By substituting equations (3) and (1) into equation (2), integrating equation (2) by parts and accounting for the static equilibrium configuration, the following non-linear partial differential equations governing the planar motion of a suspended cable are obtained:

$$\frac{\partial}{\partial x}\left\{EA\left[\frac{\partial u}{\partial x} + \frac{\mathrm{d}y}{\mathrm{d}x}\frac{\partial v}{\partial x} + \frac{1}{2}\left(\frac{\partial v}{\partial x}\right)^2\right]\right\} - c_x\frac{\partial u}{\partial t} = m\frac{\partial^2 u}{\partial t^2}, \tag{4a}$$

$$\frac{\partial}{\partial x}\left\{T\frac{\partial v}{\partial x} + EA\left(\frac{\mathrm{d}y}{\mathrm{d}x} + \frac{\partial v}{\partial x}\right)\left[\frac{\partial u}{\partial x} + \frac{\mathrm{d}y}{\mathrm{d}x}\frac{\partial v}{\partial x} + \frac{1}{2}\left(\frac{\partial v}{\partial x}\right)^2\right]\right\} + f(x,t) - c_y\frac{\partial v}{\partial t} = m\frac{\partial^2 v}{\partial t^2}. \tag{4b}$$

In the dynamic configuration, the total tension in the cable is $T_t = T + h(t)$, where $h(t)$ is the additional tension due to vibration and is given by

$$h(t) = EA\left[\frac{\partial u}{\partial x} + \frac{\mathrm{d}y}{\mathrm{d}x}\frac{\partial v}{\partial x} + \frac{1}{2}\left(\frac{\partial v}{\partial x}\right)^2\right]. \tag{5}$$

Equation (4) reduces to the motion equation of a taut string by letting $y(x) \equiv 0$, and gives rise to the linear motion equations of a suspended cable with initial sag by eliminating the non-linear terms $(\partial v/\partial x)^2$ and $(\partial u/\partial x)\,(\partial v/\partial x)$.

2.2. SPATIAL DISCRETIZATION

The finite-difference method is applied for the spatial discretization of equation (4). As shown in Figure 2, the cable length is equally distanced by $(n + 1)$ nodes with $s_0 = 0$ and $s_n = L$. The interval distance between the ith and $(i + 1)$th nodes is $\Delta l = L_x/n$. Using the central difference algorithm, the derivatives of the dynamic displacement components u and

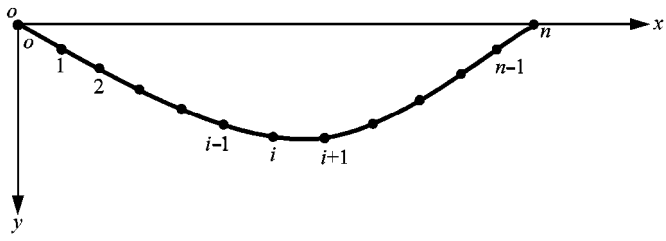

Figure 2. Schematic of equally distanced nodes.

v at the ith node an be expressed as

$$\left.\frac{\partial u}{\partial x}\right|_{x=x_i} = \frac{u_{i+1} - u_{i-1}}{2\Delta l}, \quad \left.\frac{\partial^2 u}{\partial x^2}\right|_{x=x_i} = \frac{u_{i+1} - 2u_i + u_{i-1}}{\Delta l^2}, \tag{6a,b}$$

$$\left.\frac{\partial v}{\partial x}\right|_{x=x_i} = \frac{v_{i+1} - v_{i-1}}{2\Delta l}, \quad \left.\frac{\partial^2 v}{\partial x^2}\right|_{x=x_i} = \frac{v_{i+1} - 2v_i + v_{i-1}}{\Delta l^2}. \tag{6c,d}$$

Substituting equation (6) into equation (4) yields the following ordinary differential equations:

$$\begin{aligned}&\frac{1}{\Delta l^2}(u_{i+1} - 2u_i + u_{i-1}) + \frac{y_i''}{2\Delta l}(v_{i+1} - v_{i-1}) + \frac{y_i'}{\Delta l^2}(v_{i+1} - 2v_i + v_{i-1})\\ &\quad + \frac{1}{2\Delta l^3}(v_{i+1}^2 - 2v_{i+1}v_i + 2v_iv_{i-1} - v_{i-1}^2) = \frac{m}{EA}\frac{\partial^2 u_i}{\partial t^2} + \frac{c_x}{EA}\frac{\partial u_i}{\partial t},\end{aligned} \tag{7a}$$

$$\begin{aligned}&\frac{y_i''}{2\Delta l}(u_{i+1} - u_{i-1}) + \frac{y_i'}{\Delta l^2}(u_{i+1} - 2u_i + u_{i-1})\\ &\quad + \frac{1}{\Delta l^3}(u_{i+1}v_{i+1} - u_{i+1}v_i - u_iv_{i+1} + u_iv_{i-1} + u_{i-1}v_i - u_{i-1}v_{i-1})\\ &\quad + \left(\frac{T_i'}{2EA\Delta l} + \frac{y_i'y_i''}{\Delta l}\right)(v_{i+1} - v_{i-1}) + \left[\frac{T_i}{EA\Delta l^2} + \frac{(y_i')^2}{\Delta l^2}\right](v_{i+1} - 2v_i + v_{i-1})\\ &\quad + \frac{3y_i''}{8\Delta l^2}(v_{i+1}^2 - 2v_{i+1}v_{i-1} + v_{i-1}^2) + \frac{3y_i'}{2\Delta l^3}(v_{i+1}^2 - 2v_{i+1}v_i + 2v_iv_{i-1} - v_{i-1}^2)\\ &\quad + \frac{3}{8\Delta l^4}(v_{i+1}^3 - 2v_{i+1}^2v_i - v_{i+1}^2v_{i-1} + 4v_{i+1}v_iv_{i-1} - v_{i+1}v_{i-1}^2 - 2v_iv_{i-1}^2 + v_{i-1}^3)\\ &\quad + \frac{f(x_i, t)}{EA} = \frac{m}{EA}\frac{\partial^2 v_i}{\partial t^2} + \frac{c_y}{EA}\frac{\partial v_i}{\partial t} \quad (i = 1, 2, \ldots, n-1).\end{aligned} \tag{7b}$$

Equation (7) involves quadratic and cubic non-linear terms, and therefore cannot be solved directly by the Laplace transform technique.

3. PRESENTATION OF METHOD

An iterative scheme involving the combined use of the pseudo-force method and the Laplace transform technique is presented to solve for equation (7). In order to obtain a pseudo-linear system, the non-linear effects in equation (7) are defined as pseudo-forces

$$P_{ix}(t) = \frac{EA}{2\Delta l^3}(v_{i+1}^2 - 2v_{i+1}v_i + 2v_iv_{i-1} - v_{i-1}^2), \tag{8a}$$

$$\begin{aligned} P_{iy}(t) = {} & \frac{EA}{\Delta l^3}(u_{i+1}v_{i+1} - u_{i+1}v_i - u_iv_{i+1} + u_iv_{i-1} + u_{i-1}v_i - u_{i-1}v_{i-1}) \\ & + \frac{3EAy_i''}{8\Delta l^2}(v_{i+1}^2 - 2v_{i+1}v_{i-1} + v_{i-1}^2) \\ & + \frac{3EAy_i'}{2\Delta l^3}(v_{i+1}^2 - 2v_{i+1}v_i + 2v_iv_{i-1} - v_{i-1}^2) \\ & + \frac{3EA}{8\Delta l^4}(v_{i+1}^3 - 2v_{i+1}^2v_i - v_{i+1}^2v_{i-1} + 4v_{i+1}v_iv_{i-1} \\ & - v_{i+1}v_{i-1}^2 - 2v_iv_{i-1}^2 + v_{i-1}^3) \quad (i = 1, 2, \ldots, n-1). \end{aligned} \tag{8b}$$

$P_{ix}(t)$ and $P_{iy}(t)$ are the pseudo-force components applied at the ith node in the longitudinal and vertical directions respectively. With the estimated response values in the previous iteration, the pseudo-forces are evaluated in the time domain and then treated as external forces in the next iteration. In this way, at the kth iterative step equation (7) can be represented by the following linearized equations:

$$\begin{aligned} & m\frac{\partial^2 u_i^{(k)}}{\partial t^2} + c_x\frac{\partial u_i^{(k)}}{\partial t} + a_{i1}u_{i-1}^{(k)} + a_{i2}v_{i-1}^{(k)} + a_{i3}u_i^{(k)} + a_{i4}v_i^{(k)} \\ & \quad + a_{i5}u_{i+1}^{(k)} + a_{i6}v_{i+1}^{(k)} = P_{ix}^{(k-1)}(t), \end{aligned} \tag{9a}$$

$$\begin{aligned} & m\frac{\partial^2 v_i^{(k)}}{\partial t^2} + c_y\frac{\partial v_i^{(k)}}{\partial t} + b_{i1}u_{i-1}^{(k)} + b_{i2}v_{i-1}^{(k)} + b_{i3}u_i^{(k)} + b_{i4}v_i^{(k)} + b_{i5}u_{i+1}^{(k)} + b_{i6}v_{i+1}^{(k)} \\ & \quad = P_{iy}^{(k-1)}(t) + f(x_i, t) \quad (i = 1, 2, \ldots, n-1) \end{aligned} \tag{9b}$$

in which the expressions of the coefficients a_i and b_i are given in Appendix A.

Equation (9) is solved by the Laplace transform technique. Because the dynamic loads exerted on the cable, e.g., the wind and earthquake excitations, are complicated functions of time usually given in a discrete form, the direct and inverse Laplace transforms can only be evaluated using numerical approaches. There are numerous methods available for the numerical Laplace transform [29, 30]. In the present study, the Wilcox method [31] is adopted due to its several advantages [32]. Following the Wilcox method, the discrete Laplace transform pair is formulated in a manner similar to the discrete Fourier

transform pair as

$$\tilde{f}(p_l) = \frac{T}{2N} \sum_{m=1}^{2N} [\mathrm{e}^{\gamma t_m} f(t_m)]\, \mathrm{e}^{-\mathrm{j}(2l-1)(2m-1)\pi/4N}, \tag{10a}$$

$$f(t_m) = \frac{2}{T} \mathrm{e}^{\gamma t_m} \mathrm{Re}\left[\sum_{l=1}^{N} \tilde{f}(p_l)\, \mathrm{e}^{\mathrm{j}(2l-1)(2m-1)\pi/4N} \right], \tag{10b}$$

where $p_l = \gamma + \mathrm{j}(2l-1)\pi/T (l = 1, 2, \ldots, N)$ is the discrete Laplace transform parameter, j is the imaginary unit, T is the time duration of interest in the transient analysis, N is the number of equi-spaced sampling intervals in $[0, T]$, and $t_m = (2m-1)T/(4N) (m = 1, 2, \ldots, 2N)$ is the discrete-time parameter.

Equation (10) can be regarded as the discrete Fourier transform of $f(t)$ with a window function $\mathrm{e}^{-\gamma t}$. Therefore, by taking N to be an integer power of 2 and using an appropriate empirical rule in determining the transform parameters, the numerical Laplace forward and inverse transforms in equation (10) can be directly and efficiently computed by utilizing the FFT algorithm. In the computation of numerical Fourier transform, the coefficient γ is taken as $2\pi/T$ according to Wilcox [31].

Taking the Laplace transform of equation (9) with respect to time yields

$$\begin{aligned} &m[\, p^2\tilde{u}_i - pu_i(0) - \dot{u}_i(0)] + c_x[\, p\tilde{u}_i - u_i(0)] \\ &\quad + a_{i1}\tilde{u}_{i-1} + a_{i2}\tilde{v}_{i-1} + a_{i3}\tilde{u}_i + a_{i4}\tilde{v}_i + a_{i5}\tilde{u}_{i+1} + a_{i6}\tilde{v}_{i+1} = \tilde{P}_{ix}(p), \end{aligned} \tag{11a}$$

$$\begin{aligned} &m[\, p^2\tilde{v}_i - pv_i(0) - \dot{v}_i(0)] + c_y[\, p\tilde{v}_i - v_i(0)] \\ &\quad + b_{i1}\tilde{u}_{i-1} + b_{i2}\tilde{v}_{i-1} + b_{i3}\tilde{u}_i + b_{i4}\tilde{v}_i + b_{i5}\tilde{u}_{i+1} + b_{i6}\tilde{v}_{i+1} = \tilde{P}_{iy}(p) + \tilde{f}(x_i, p) \\ &\quad (i = 1, 2, \ldots, n-1). \end{aligned} \tag{11b}$$

The time-dependent terms in equation (9) have been removed by transforming to the Laplace domain. Equation (11) can be re-arranged for computational convenience in the following form:

$$\begin{aligned} &a_{i1}\tilde{u}_{i-1} + a_{i2}\tilde{v}_{i-1} + (a_{i3} + mp^2 + c_x p)\tilde{u}_i + a_{i4}\tilde{v}_i + a_{i5}\tilde{u}_{i+1} + a_{i6}\tilde{v}_{i+1} \\ &\quad = m[\, pu_i(0) + \dot{u}_i(0)] + c_x u_i(0) + \tilde{P}_{ix}(p), \end{aligned} \tag{12a}$$

$$\begin{aligned} &b_{i1}\tilde{u}_{i-1} + b_{i2}\tilde{v}_{i-1} + b_{i3}\tilde{u}_i + (b_{i4} + mp^2 + c_y p)\tilde{v}_i + b_{i5}\tilde{u}_{i+1} + b_{i6}\tilde{v}_{i+1} \\ &\quad = m[\, pv_i(0) + \dot{v}_i(0)] + c_y v_i(0) + \tilde{P}_{iy}(p) + \tilde{f}(x_i, p) \quad (i = 1, 2, \ldots, n-1). \end{aligned} \tag{12b}$$

With the given Laplace domain parameter p, equation (12) constitutes linear algebraic equations with respect to the unknowns $\tilde{u}_{i-1}, \tilde{v}_{i-1}, \tilde{u}_i, \tilde{v}_i, \tilde{u}_{i+1}, \tilde{v}_{i+1} (i = 1, 2, \ldots, n-1)$. In recognizing $u_0 = v_0 = u_n = v_n = 0$ due to the fixed ends, we can eliminate the variables $\tilde{u}_0$, $\tilde{v}_0$, $\tilde{u}_n$, $\tilde{v}_n$ from the equations. By defining

$$\{\tilde{\mathbf{u}}\} = \{\tilde{u}_1\ \tilde{v}_1\ \cdots\ \tilde{u}_i\ \tilde{v}_i\ \cdots\ \tilde{u}_{n-1}\ \tilde{v}_{n-1}\}^{\mathrm{T}} \tag{13}$$

a system of $2(n-1)$ linear complex algebraic equations in the transformed domain is obtained from equation (12) as

$$[\mathbf{D}]\{\tilde{\mathbf{u}}\} = \{\tilde{\mathbf{F}}\} \tag{14}$$

in which the coefficient matrix $[\mathbf{D}]$, the force vector $\{\tilde{\mathbf{F}}\}$ and the solution vector $\{\tilde{\mathbf{u}}\}$ are all complex-valued quantities. Equation (14) can be solved by directly using complex operation or through transformation into real algebraic equations. Appendix B presents in detail the derivation and expressions of transforming equation (14) into a system of $4(n-1)$ linear real algebraic equations with the separated real and imaginary components of the node displacements in the Laplace domain as unknowns. The direct Gaussian elimination method is used to solve the real algebraic equations in the present study.

When the transformed displacements $\{\tilde{\mathbf{u}}\}$ are solved from equation (14), the time-domain displacement responses at the present iteration are obtained by numerical inversion of the Laplace solution. They are used to update the pseudo-forces for all values of time in the next iteration and then transformed to the Laplace domain where the quasi-linear equations of motion are solved. This process is repeated iteratively until the difference of evaluated responses between two consecutive iterations is small enough.

4. IMPLEMENTATION ISSUES

Because the proposed method requires the iteration to be carried out simultaneously for all values of the time duration of interest in the transient response analysis, the iteration may not converge—within the given tolerance—when the time duration is long. The segmenting technique [26] is introduced here to improve the convergence. Following this approach, the entire time duration of interest is divided into several time segments T_i ($i = 1, 2, \ldots, M$), each consisting of a certain number of time steps. The iteration is then implemented segment by segment. Because the response at time t_i is not influenced by the exciting force exerted at $t > t_i$, the pseudo-forces for $t > t_i$ are imposed constantly to zero when computing the time segment with the terminal instant t_i. At the same time, the pseudo forces at the previous time segments, which have reached convergence before, should be kept unvaried in the iterative computation for the present segment. So the pseudo-forces are updated only within the concerned iteration segment. The iteration convergence can be ensured when an appropriate number of time segments are selected [26]. In contrast to the HFTD procedure [27], the proposed method does not need a decaying loading function to append the exciting forces and the pseudo-forces at the end of each segment.

Since there is a tendency for the time function to "break up" as $t \to T$ when applying the Wilcox method for numerical Laplace inversion, Wilcox [31] suggested that the time span used in numerical Laplace transform should be slightly larger than the actual time duration so as to make allowance for this phenomenon. In the present practice, given the time duration of interest for transient response analysis T, the time span of numerical Laplace transform is taken to be $T' = \alpha T$ with α being about 1·2, and the transform results obtained for $t > T$ are discarded.

The algorithm of the proposed hybrid pseudo-force/Laplace transform method for the cable dynamic analysis is summarized in the following steps:

1. Determine the time duration for transient response analysis T and the number of spatial discretization nodes n. Given the time span factor α, the time segment number M, the tolerance ε, and the allowable iterative number N. Let $k = 0$.

2. Compute the transformed dynamic loads $\{\tilde{\mathbf{f}}(p)\}$ from $f(x, t)$ within the time span $[0, T']$ by using the numerical forward Laplace transform. Solve equation (14) by assuming zero pseudo-forces to obtain the transformed displacement responses of the linear problem.
3. Transform the Laplace solutions by using the numerical inversion to obtain the linear displacement responses in the time domain. Take these linear responses as initial guesses $\{\mathbf{u}^{(0)}\}$ and repeat the following steps with $k = 1, 2, \ldots$ and $i = 1, 2, \ldots, M$.
4. Compute the pseudo-forces $\{\mathbf{P}_x(\mathbf{u}^{(k-1)})\}$ and $\{\mathbf{P}_y(\mathbf{u}^{(k-1)})\}$ from equation (8) and only those within the ith time segment T_i being iterated currently are updated. Solve equation (14) with updated pseudo-forces to obtain the transformed displacement responses $\{\tilde{\mathbf{u}}^{(k)}\}$.
5. Transform the Laplace solutions $\{\tilde{\mathbf{u}}^{(k)}\}$ by use of the numerical inversion to obtain the time-domain displacement responses at the present iteration. If $\sum_j \|\mathbf{u}^{(k)}(t_j) - \mathbf{u}^{(k-1)}(t_j)\|_{t_j \in T_j} \leqslant \varepsilon$, obtain the solutions in the ith time segment and go to the $(i + 1)$th segment iteration until the Mth time segment is reached.
6. If $\sum_j \|\mathbf{u}^{(k)}(t_j) - \mathbf{u}^{(k-1)}(t_j)\|_{t_j \in T_j} > \varepsilon$ and $k < N$, set $k := k + 1$ and return to step 4. Otherwise re-divide the ith time segment into N_i sub-segments and iterate each sub-segment until convergence. Otherwise re-divide the ith time segment into N_i sub-segments and iterate each sub-segment until convergence.

5. ILLUSTRATIVE EXAMPLES

5.1. EXAMPLE 1: A SHORT CABLE

A relatively short suspended cable (Cable I) with the horizontal span $L_x = 329{\cdot}2$ m and the sag $d = 5{\cdot}81$ m is first analyzed. This cable has the modulus of elasticity $E = 2{\cdot}0 \times 10^{11}$ Pa, the cross-sectional area $A = 0{\cdot}759\ \text{m}^2$, the mass per unit length $m = 5951{\cdot}04$ kg/m, and the horizontal tension $T_x = 1{\cdot}388 \times 10^5$ kN. The cable natural frequencies of in-plane modes are given in Table 1. The primary critical damping of the cable is estimated to be $\xi = 0{\cdot}5\%$. The corresponding damping constant c is obtained by the formula [33]

$$c = 2\zeta \sqrt{EAm}. \tag{15}$$

Cable I is divided into 18 elements in the analysis, i.e., $n = 18$. The damped free vibration of the cable is first evaluated. The initial transverse displacement along the

TABLE 1

Natural frequencies of in-plane modes of Cable I

Mode order	Natural frequency (Hz)	Remark
1	0·3830	Symmetric mode
2	0·4642	Antisymmetric mode
3	0·7066	Symmetric mode
4	0·9321	Antisymmetric mode
5	1·1741	Symmetric mode
6	1·4223	Antisymmetric mode

cable is taken as

$$v_0(x) = s_0 \sin(\pi x/L_x) \tag{16}$$

with $s_0 = 1{\cdot}5$ m.

The transient response solution is initially tried by taking the entire time duration of interest of 70 s as one time segment, but the iteration fails to converge. Subsequently, the solution process is repeated by arbitrarily dividing the time duration into 18 segments, each consisting of 50 time steps. The iteration is performed segment by segment and the convergence is reached for all segments. Figure 3(a) shows the predicted displacement response at the cable mid-span. In all the figures throughout this paper, the positive

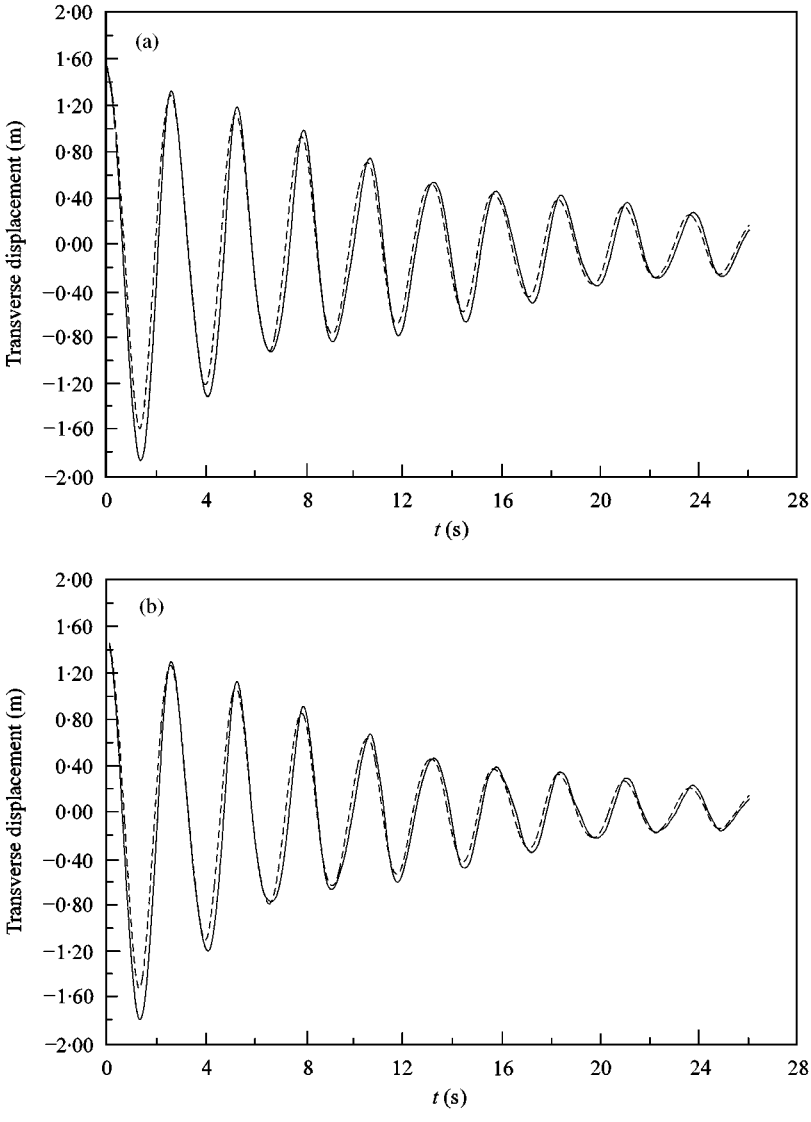

Figure 3. Transverse displacement response at mid-span under free vibration: (a) critical damping $\xi = 0{\cdot}5\%$; (b) critical damping $\xi = 0{\cdot}6\%$. —— Non-linear, – – – linear.

response indicates the "moving-down" displacement and the negative response indicates the "moving-up" displacement. In order to check if the system damping influences the iteration convergence, the response solution is tried again by taking the entire time duration as one time segment but increasing the critical damping from 0·5 to 0·6%. In this case, the iteration convergence is achieved and the computation results are given in Figure 3(b). It is shown that the convergence is indeed influenced by the system damping. When the damping is low, we should use quite a number of time segments to reach convergence.

Both the linear and non-linear responses are illustrated in Figure 3 for comparison. There is a frequency shift of the non-linear solution relative to the linear solution. As the non-linear response amplitudes occur behind the corresponding linear response amplitudes, this cable exhibits softening non-linearity. In fact, the geometric non-linearities of the

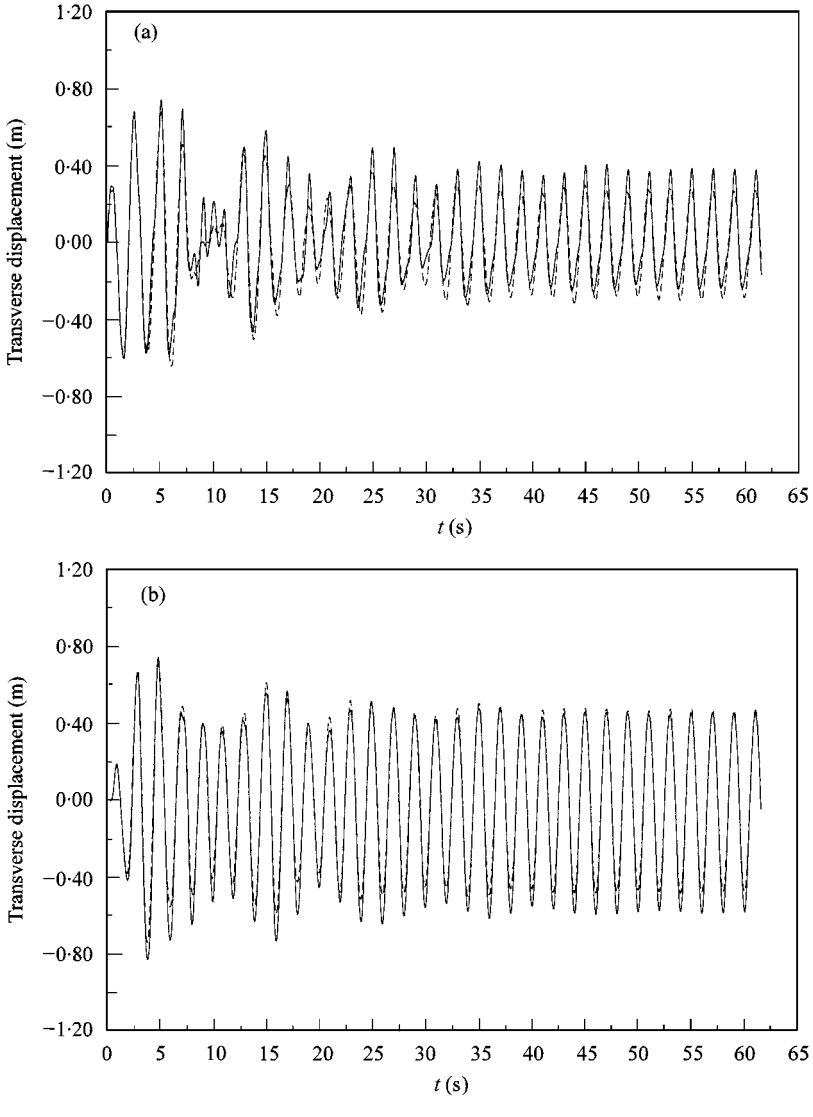

Figure 4. Transverse displacement response under concentrated harmonic excitation with $f = 0{\cdot}5$ Hz: (a) at mid-span; (b) at quarter-span. —— Non-linear, – – – linear.

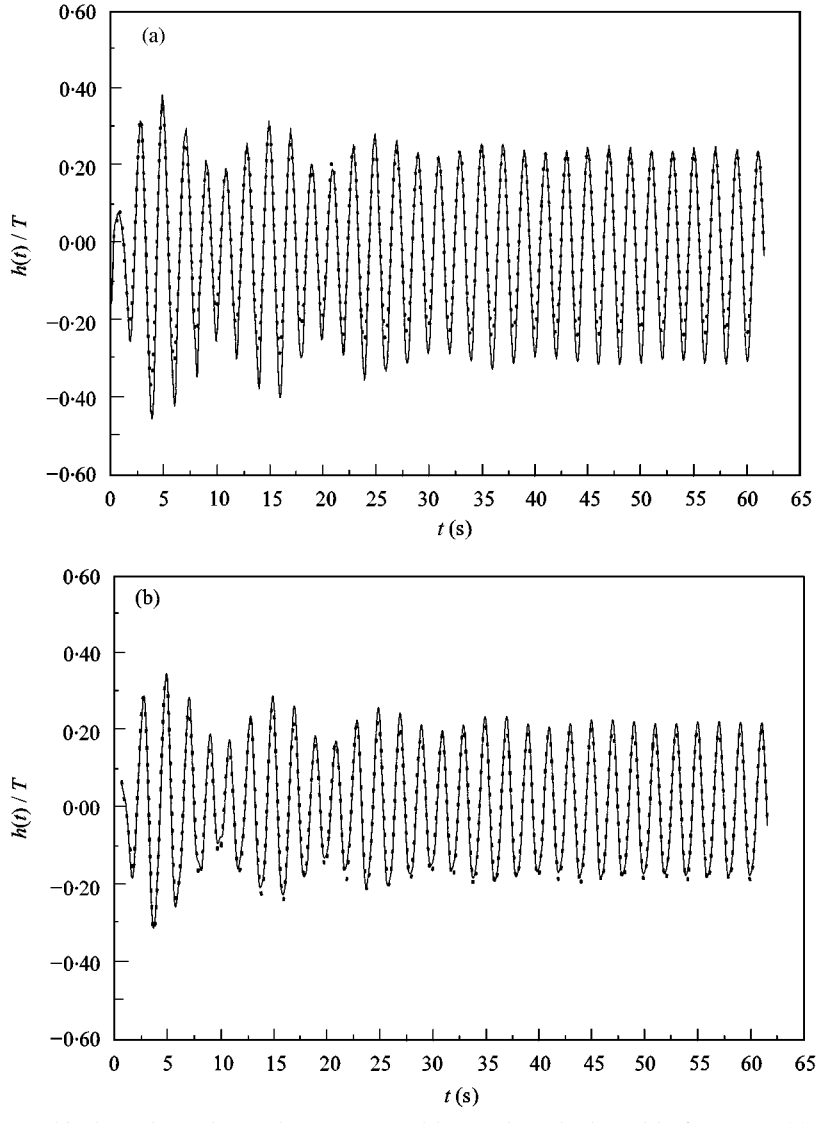

Figure 5. Cable dynamic tension under concentrated harmonic excitation with $f = 0{\cdot}5$ Hz: (a) at mid-span; (b) at quarter-span. —— Non-linear, – – – linear.

cable include quadratic and cubic non-linearities. Both softening and hardening behaviours may occur depending on the relative contributions of the quadratic and cubic non-linearities that are concerned with the cable parameters (e.g., sag, static tension) and vibration mode.

The dynamic responses of Cable I subjected to a concentrated vertical harmonic excitation at mid-span are then analyzed. The harmonic excitation is in the form

$$F = F_0 \cos(2\pi f t), \tag{17}$$

where F_0 is the exciting force amplitude and f is the excitation frequency. In this example, the force amplitude is $F_0 = 1{\cdot}6 \times 10^3$ kN, and the excitation frequency f is taken to be 0·5

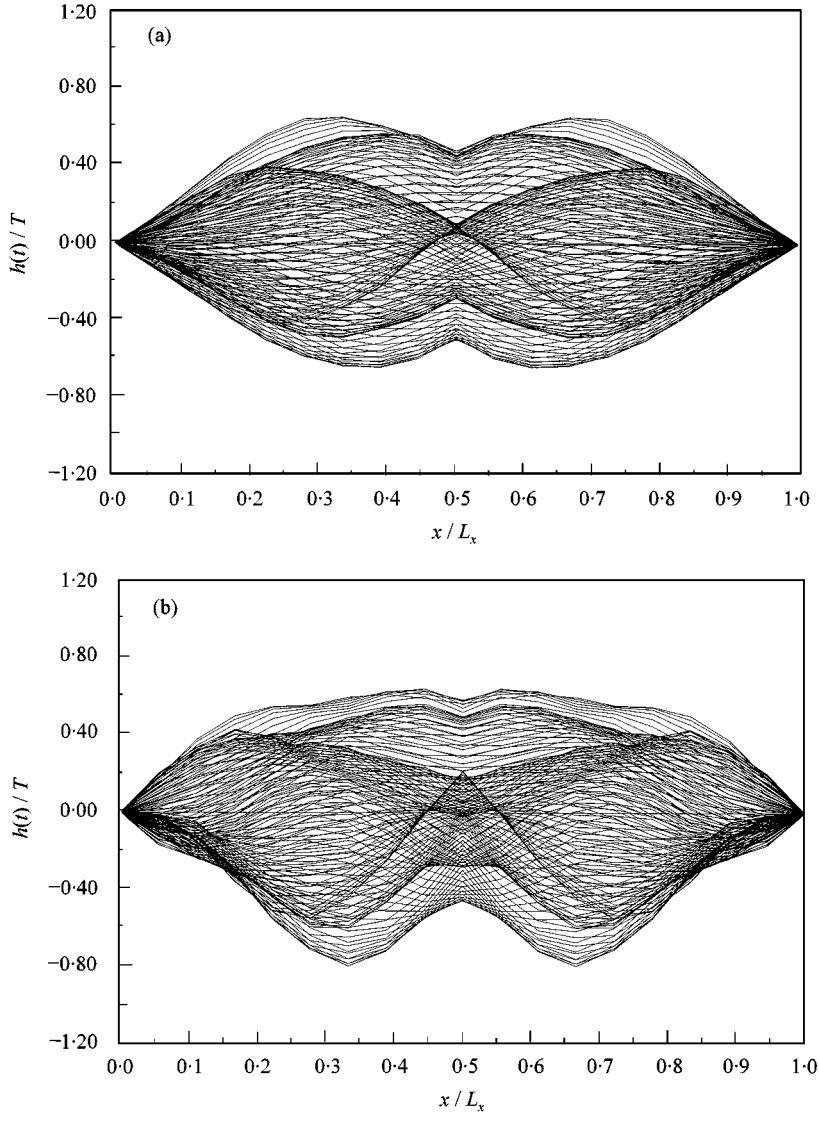

Figure 6. Transverse vibration profile at different instants ($t = 10$–15 s) under concentrated harmonic excitation: (a) linear; (b) non-linear.

and 0·19 Hz respectively. The cable (static) tension is reduced to 90% of the original value ($1{\cdot}388 \times 10^5$ kN) and the static configuration is accordingly updated to investigate the non-linearity effects at a lower tension. In order to quickly accomplish the iteration at each time segment, the entire time duration of 150 s is divided into 300 segments, each consisting of six time steps.

Figures 4–7 give the analysis results for $f = 0{\cdot}5$ Hz. Figure 4 shows the transverse displacement response at the mid-span and at the quarter-span respectively. It is seen that the non-linearities result in a quasi-static displacement drift to the down-position (positive displacement drift) at the mid-span and to the up-position (negative displacement drift) at the quarter-span. With the displacement response time history, the cable dynamic

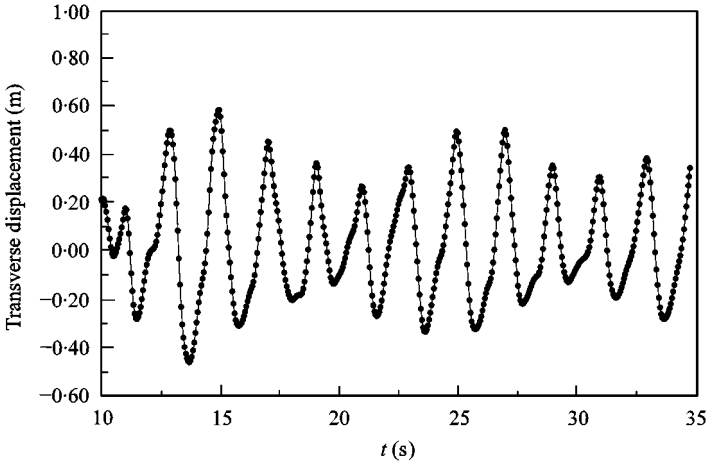

Figure 7. Comparison of predicted responses at mid-span by the proposed method and the Runge–Kutta method: —present method; ● Runge–Kutta method.

tension can be readily evaluated from equation (5). Figure 5 gives the ratio of dynamic tension to initial static tension at the mid-span and at the quarter-span respectively. It is observed that the non-linearities give rise to a negative tension drift (compressing) at the mid-span and a positive tension drift (tensioning) at the quarter-span. Figure 6 illustrates, respectively, the linear and non-linear transverse vibration profiles at different instants from $t = 10$ to 15 s. It is seen that the non-linear vibration profile is much more complicated in the spatial shape than the corresponding linear vibration profile. This explains why the conventional procedure by making use of a few linearized modal deflection functions cannot provide accurate non-linear response prediction in some circumstances.

In this example, a numerical verification is also carried out by evaluating the non-linear dynamic response using the proposed method and using the sixth order Runge–Kutta method. Figure 7 shows a comparison of these results, where the solid line indicates the response results of the proposed method, while the circle points denote the result of the Runge–Kutta method. It is seen that the results of the present method are in close agreement with the Runge–Kutta integration results.

Figure 8 and 9 give the analysis results when the frequency of the harmonic excitation is taken as $f = 0{\cdot}19$ Hz. The transverse displacement response at the mid-span and at the quarter-span is shown in Figure 8. It is observed that, in contrast to the case of $f = 0{\cdot}5$ Hz, the non-linear displacement response now exhibits a quasi-state drift to the up-position (negative displacement drift) at the mid-span. At the quarter-span, the displacement drift is still in the up-position but the response contains high-frequency components. These results indicate that the non-linear dynamic response under a simple harmonic excitation may produce positive or negative drift depending on the exciting frequency, and may exhibit significant multi-harmonic response components even in the steady state. Figure 9 shows the ratio of dynamic tension to initial static tension at the mid-span and at the quarter-span. It is seen that the dynamic tension taking into account non-linearity is obviously larger than the corresponding dynamic tension without considering non-linearity and accommodates multi-harmonic components.

An advantage of the proposed method is that it can directly deal with a system with viscoelastic damping parametrically dependent on the frequency parameter or

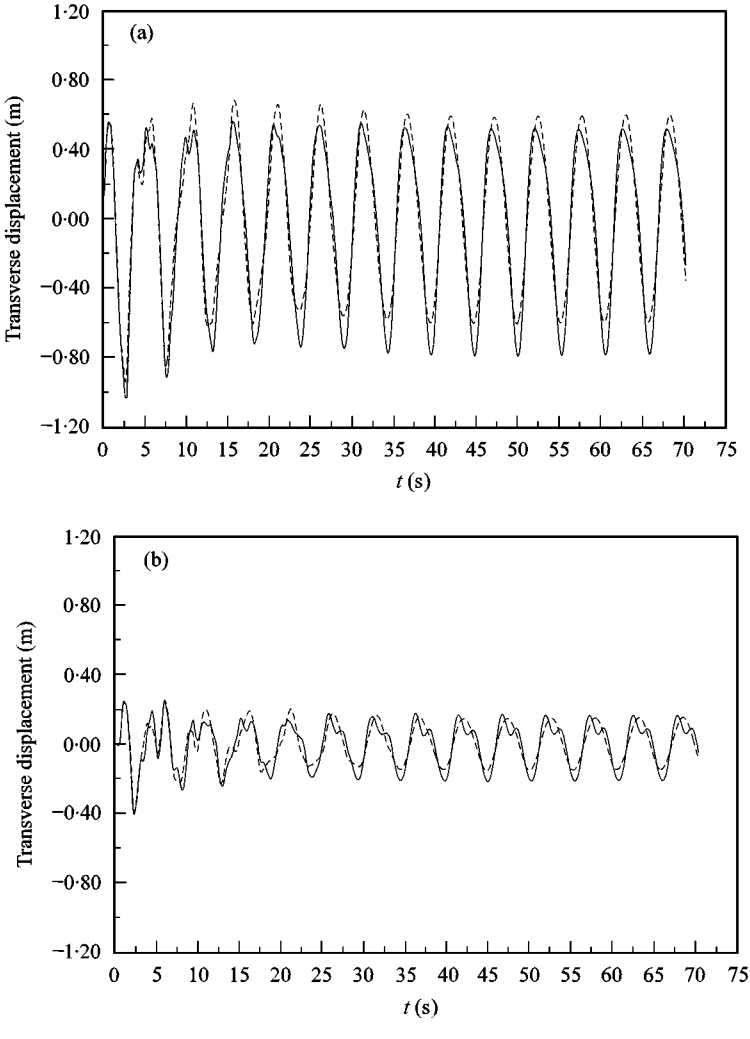

Figure 8. Transverse displacement response under concentrated harmonic excitation with $f = 0{\cdot}19$ Hz: (a) at mid-span; (b) at quarter-span. —— Non-linear, – – – linear.

with linear hysteretic damping (complex damping). It has been revealed that the cable damping mainly stems from the internal friction damping due to flexure hysteresis [34]. As an example, the transient response of Cable I with complex damping is analyzed by the proposed method. The complex damping is introduced by replacing E with $E(1 + \mathrm{j}\eta)$ and letting $c = 0$. Figure 10(a) shows the transverse displacement response at the mid-span of Cable I with complex damping ($\eta = 0{\cdot}06$) subjected to the following quasi-static loading:

$$F(kN) = \begin{cases} 2{\cdot}5 \times 10^3 t & \text{for } 0 \leqslant t \leqslant 1{\cdot}0, \\ 2{\cdot}5 \times 10^3 & \text{for } t > 1{\cdot}0. \end{cases} \tag{18}$$

It is observed from Figure 10(a) that since the complex damping essentially degrades the primary modal oscillations, the response retains high-frequency components and decay of

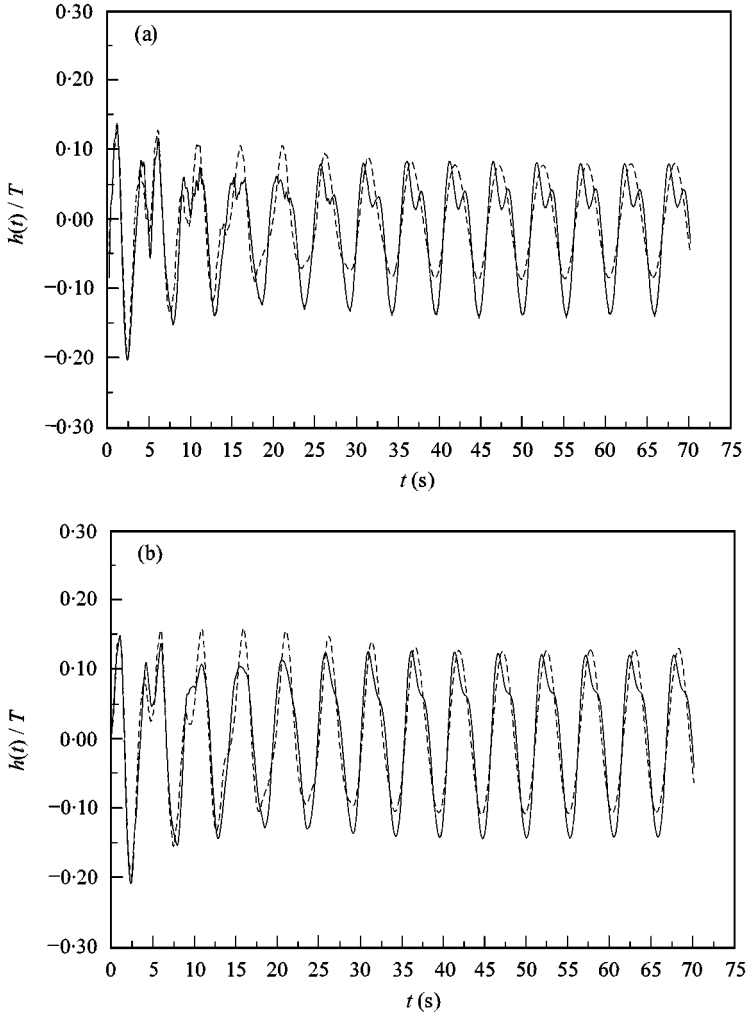

Figure 9. Cable dynamic tension under concentrated harmonic excitation with $f = 0{\cdot}19$ Hz: (a) at mid-span; (b) at quarter-span. —— Non-linear, – – – linear.

the vibration to a static response takes a long time. As a comparison, Figure 10(b) gives the response of Cable I with viscous damping ($\xi = 0{\cdot}5\%$) under the same quasi-static loading. With the viscous damping, the response evolves like damped free vibration in the primary period, and decays quickly to a static response. The non-linear static response is smaller than the linear static response in both complex damping and viscous damping cases.

5.2. EXAMPLE 2: TSING MA BRIDGE CABLE

The main-span suspended cable of the Tsing Ma Bridge with a 1377 m main span, referred to as Cable II, is analyzed as a long-span cable example. The field measurements of modal properties of the suspension Tsing Ma Bridge at a series of construction stages have been conducted by ambient vibration survey [35], including the cable free hanging stage at which only the tower-cable system was erected but no deck units had been hoisted into

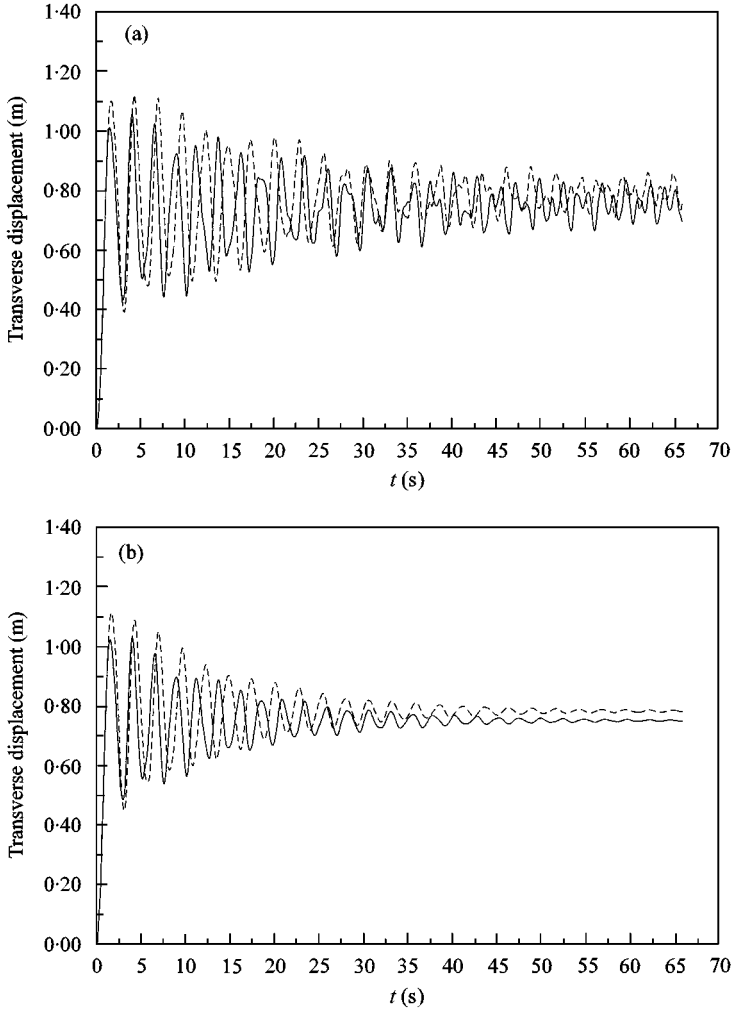

Figure 10. Transverse displacement response at mid-span under quasi-static loading: (a) complex damping ($\eta = 0{\cdot}06$); (b) viscous damping ($\xi = 0{\cdot}5\%$). —— Non-linear, – – – linear.

position. In the free hanging stage the main-span suspended cable is configured by the following parameters: the cable horizontal span $L_x = 1369{\cdot}36$ m; the sag $d = 123{\cdot}52$ m; the horizontal tension $T_x = 1{\cdot}226 \times 10^5$ kN; the modulus of elasticity $E = 2{\cdot}0 \times 10^{11}$ Pa; the cross-sectional area $A = 0{\cdot}759\ \text{m}^2$; and the mass per unit length $m = 5951{\cdot}04$ kg/m. The computed natural frequencies of in-plane modes are given in Table 2. These prediction results agree well with the measured natural frequencies of the cable. In contrast with Cable I, the first in-plane mode (and the odd-order modes) of Cable II is an antisymmetric mode. The natural frequencies of Cable II are much lower than those of Cable I due to extremely long cable span and relatively large sag. The primary viscous damping ratio is estimated to be $\xi = 0{\cdot}5\%$.

In order to verify the ability of the proposed method to deal with any type of excitations, a random dynamic loading uniformly distributed along the cable is considered. The discrete random excitation, as shown in Figure 11, is produced by using the Davenport spectrum to

TABLE 2

Natural frequencies of in-plane modes of Cable II

Mode order	Natural frequency (Hz)	Remark
1	0·1020	Antisymmetric mode
2	0·1488	Symmetric mode
3	0·2091	Antisymmetric mode
4	0·2562	Symmetric mode
5	0·3160	Antisymmetric mode
6	0·3562	Symmetric mode

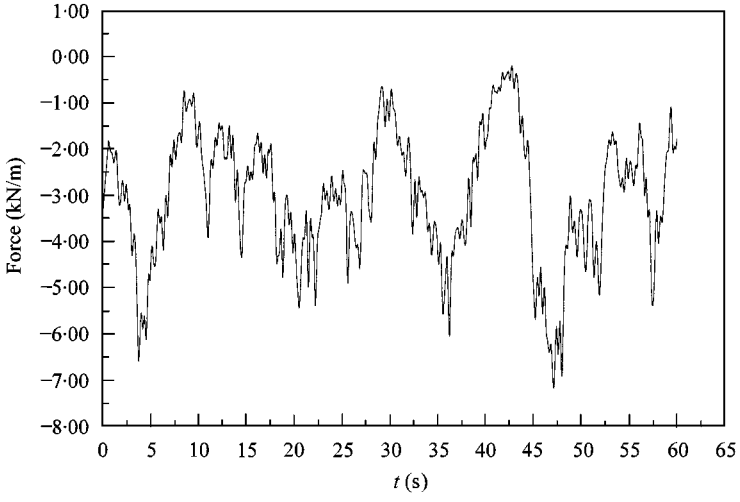

Figure 11. Time history of uniformly distributed exciting force.

simulate a wind lift load. In the response analysis, Cable II is divided into 40 elements, i.e., $n = 40$. The entire time duration of 102·4 s is portioned into 60 segments and each time segment consists of 20 steps. The iterative convergence is reached for all the time segments, and the transverse displacement response at the mid-span and at the quarter-span is shown in Figure 12. The difference of the magnitude and the phase between the non-linear and linear responses is obvious but not significant. Figure 13 shows the ratio of dynamic tension to initial static tension at the mid-span and at the quarter-span. It is seen that the additional tension caused by the cable vibration is small relative to the initial tension. Figures 14 and 15 illustrate, respectively, the transverse and longitudinal vibration profiles at different instants from $t = 50$ to 60 s. Evidently, the response profile manifests itself as a combination of the contributions from many modes. It makes clear again the necessity of containing multiple modes in non-linear transient response analysis. It is seen that during the observed time period ($t = 50 \sim 60$ s), the non-linear transverse response shows extremely large positive (moving-down) amplitudes at the locations of about $0{\cdot}15L_x$ and $0{\cdot}85L_x$, which cannot be found in the linear response. The maximum longitudinal response amplitudes also occur at about $0{\cdot}15L_x$ and $0{\cdot}85L_x$.

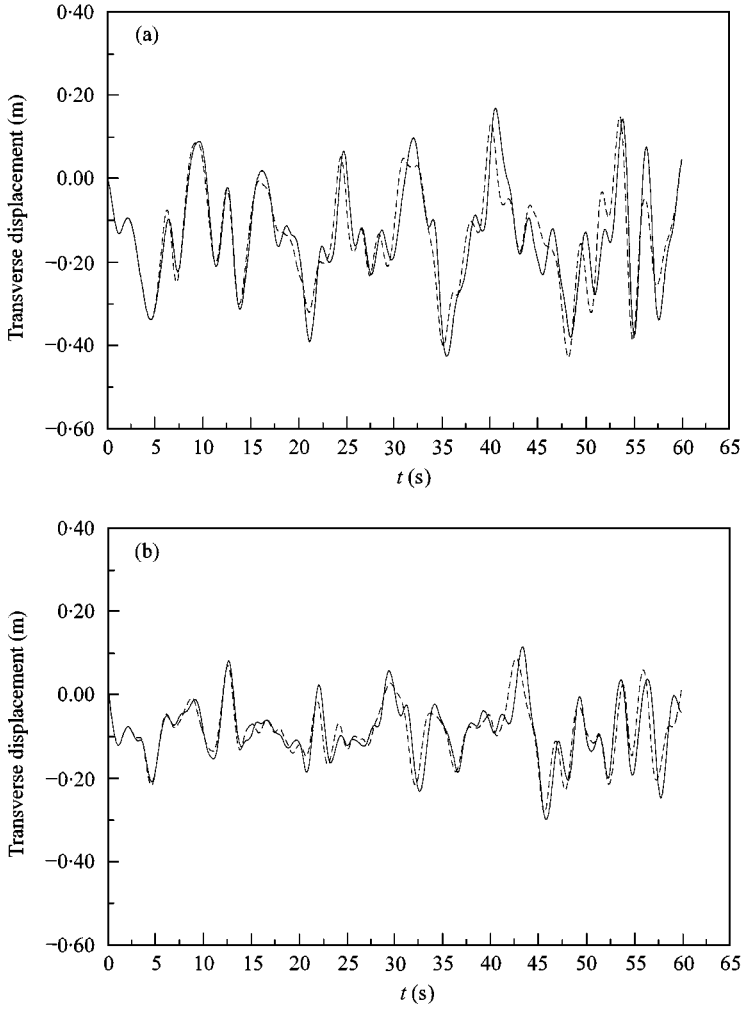

Figure 12. Transverse displacement response under uniformly distributed excitation: (a) at mid-span; (b) at quarter-span. —— Non-linear,– – – linear.

6. CONCLUSIONS

In the present study, a numerical scheme involving the hybrid application of the pseudo-force method and the Laplace transform technique in conjunction with the finite-difference discretization is presented for non-linear dynamic analysis of suspended cables under arbitrary dynamic loading. In comparison with the time-step integration method, the proposed method offers the following advantages: (1) Due to eliminating step-by-step time marching process, the method can obtain simultaneously the non-linear transient response in a time segment. It is particularly efficient in computing a long-term solution, e.g., the steady state response under periodic or quasi-static loading. (2) The proposed method can predict both the non-linear and linear transient response from one solution scheme. In fact, the linear transient response in the entire time duration of interest can be quickly evaluated by the proposed method without any iteration. (3) The proposed

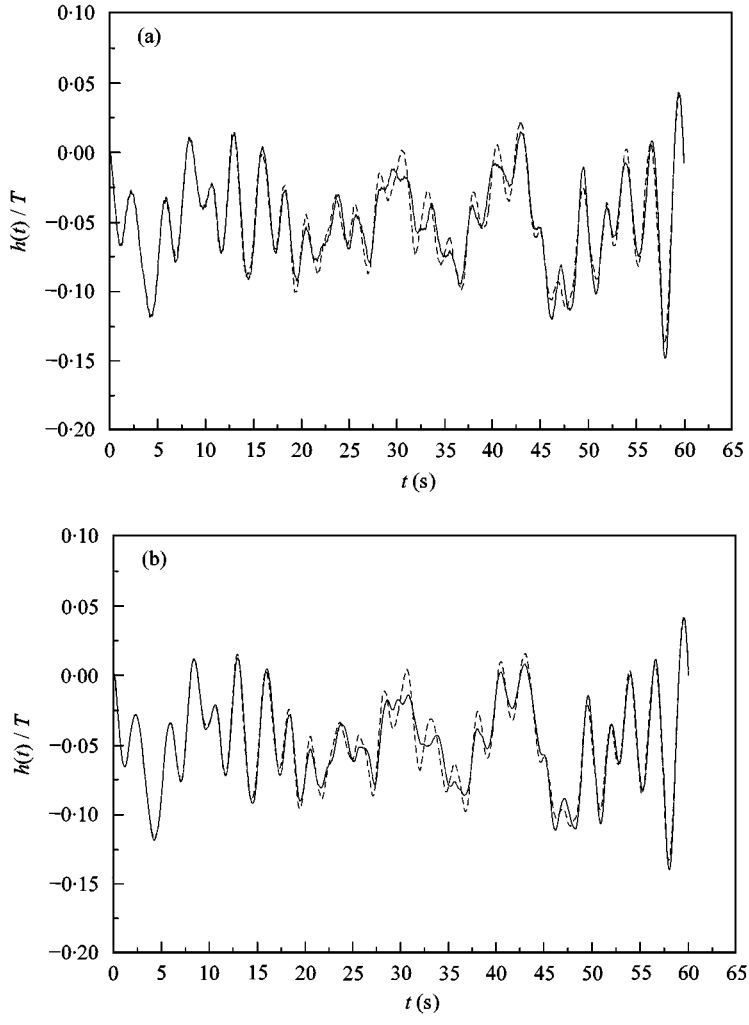

Figure 13. Cable dynamic tension under uniformly distributed excitation: (a) at mid-span; (b) at quarter-span. —— Non-linear, – – – linear.

method can readily deal with the viscoelastic damping which is parametrically dependent on frequency as well as the complex damping. It is therefore promising to extend the proposed method to the analysis of widely used cable–damper systems with viscoelastic and/or hysteretic dampers installed transversely near the cable ends.

Numerical examples including short-span and long-span cables are given to demonstrate the applicability of the proposed method. Based on the analysis results, the following conclusions on the non-linear dynamic behaviour of suspended cables are drawn: (1) Under a simple harmonic excitation, the cable non-linear oscillations (both the displacement response and the dynamic tension) are not symmetric about the equilibrium position. The displacement response (and dynamic tension) at different cable locations, may have a static drift in opposite directions (one in the up-position and another in the down-position). The static drift at the same location can also change its direction when the excitation frequency is changed. (2) The suspended cable may exhibit significant multiharmonic response

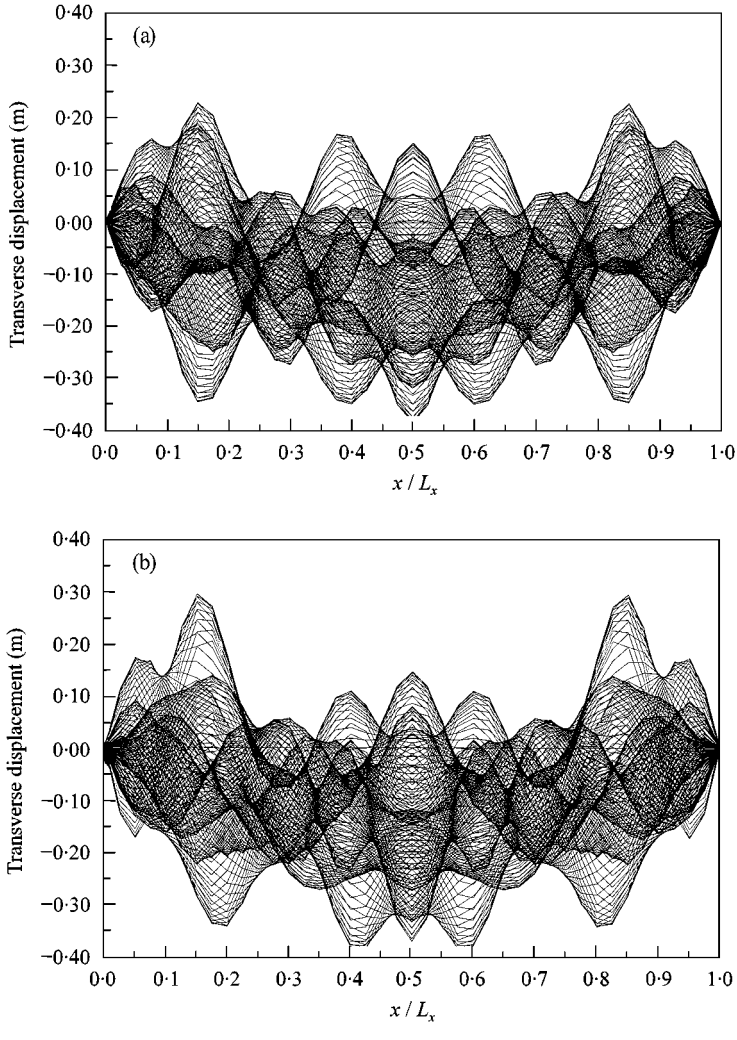

Figure 14. Transverse vibration profile at different instants (t = 50–60 s) under uniformly distributed excitation: (a) linear; (b) non-linear.

subjected to a single harmonic excitation due to the geometric non linearities. This is particularly obvious in the time history of the dynamic tension. It implies that in order to obtain steady state dynamic response, the multi-harmonic components should be accommodated in the solution scheme. (3) The non-linear vibration profile of a cable is much more complicated than the corresponding linear vibration profile even under a simple concentrated harmonic loading. When subjected to a distributed random excitation, the higher vibration models contribute significantly to the cable response. Therefore, the approximate approaches in terms of a few linearized modes usually cannot give accurate non-linear response prediction for long-span cables.

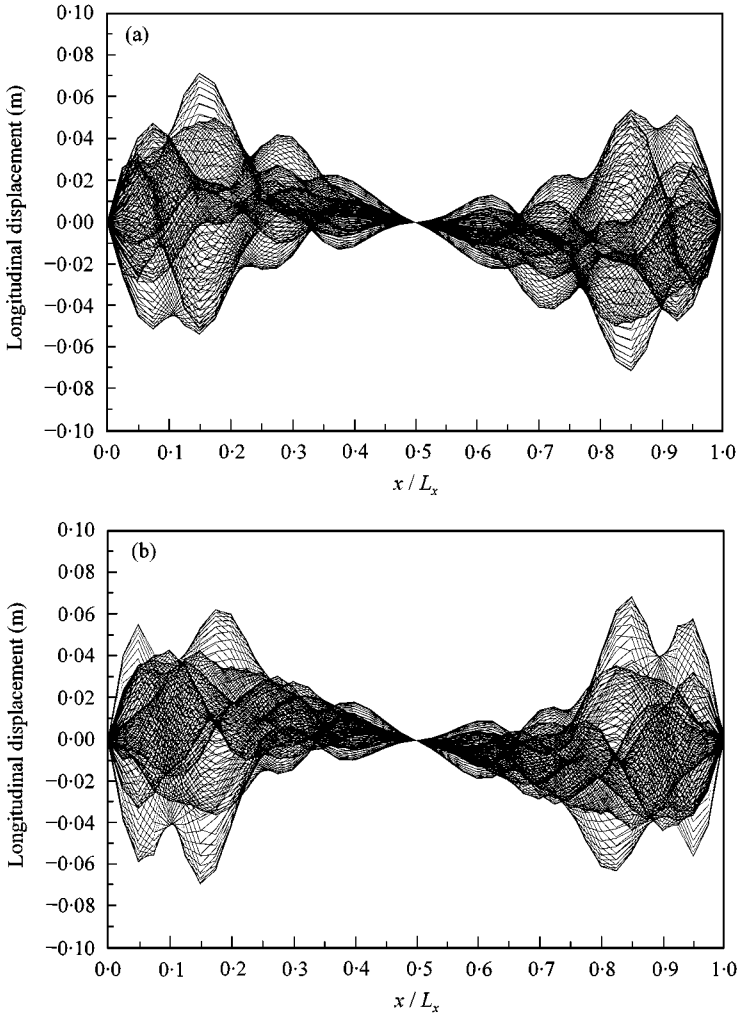

Figure 15. Longitudinal vibration profile at different instants ($t = 50$–60 s) under uniformly distributed excitation: (a) linear; (b) non-linear.

ACKNOWLEDGMENTS

This study was supported by the Hong Kong Polytechnic University under the grant G-YW29 and through the Area of Strategic Development (ASD) Programme in Structural Engineering. These supports are gratefully acknowledged.

REFERENCES

1. F. BRANCALEONI 1992 *Proceedings of the* 1*st International Symposium on Aerodynamics of Large Bridges*, *Copenhagen*, *Denmark*, 147–158. The construction phase and its aerodynamic issues.
2. H. TANAKA and N. J. GIMSING 1999 *Journal of Wind Engineering and Industrial Aerodynamics* **80**, 85–104. Aerodynamic stability of non-symmetrically erected suspension bridge girders.
3. H. M. IRVINE 1980 *Earthquake Engineering and Structural Dynamics* **8**, 267–273. The estimation of earthquake-generated additional tension in a suspended bridge cable.

4. G. V. RAO and R. N. IYENGAR 1991 *Earthquake Engineering and Structural Dynamics* **20**, 243–258. Seismic response of a long span cable.
5. K. TADA, H. JIN, M. KITAGAWA, A. NITTA and R. TORIUMI 1995 *Structural Engineering International* **5**, 179–181. Effects of the Southern Hyogo Earthquake on the Akashi-Kaikyo Bridge.
6. H. M. IRVINE and T. K. CAUGHEY 1974 *Proceedings of the Royal Society of London* **A341**, 299–315. The linear theory of free vibrations of a suspended cable.
7. P. HAGEDORN and B. SCHAFER 1980 *International Journal of Non-Linear Mechanics* **15**, 333–340. On non-linear free vibrations of an elastic cable.
8. A. LUONGO, G. REGA and F. VESTRONI 1982 *Journal of Sound and Vibration* **82**, 247–259. Monofrequent oscillations of a non-linear model of a suspended cable.
9. G. REGA, F. VESTRONI and F. BENEDETTINI 1984 *International Journal of Solids and Structures* **20**, 95–105. Parametric analysis of large amplitude free vibrations of a suspended cable.
10. S. I. AL-NOURY and S. A. ALI 1985 *Journal of Sound and Vibration* **101**, 451–462. Large-amplitude vibrations of parabolic cables.
11. F. BENEDETTINI and G. REGA 1987 *International Journal of Non-Linear Mechanics* **22**, 497–509. Non-linear dynamics of an elastic cable under planar excitation.
12. G. V. RAO and R. N. IYENGAR 1991 *Journal of Sound and Vibration* **149**, 25–41. Internal resonance and non-linear response of a cable under periodic excitation.
13. N. C. PERKINS 1992 *International Journal of Non-linear Mechanics* **27**, 233–250. Modal interactions in the non-linear response of elastic cables under parametric/external excitation.
14. F. BENEDETTINI, G. REGA and R. ALAGGIO 1995 *Journal of Sound and Vibration* **182**, 775–798. Non-linear oscillations of a four-degree-of-freedom model of a suspended cable under multiple internal resonance conditions.
15. C. LEE and N. C. PERKINS 1995 *Nonlinear Dynamics* **8**, 45–63. Three-dimensional oscillations of suspended cables involving simultaneous internal resonances.
16. X. XIAO and J. DRUEZ 1996 *Transactions of the Canadian Society for Mechanical Engineering* **20**, 123–137. Planar nonlinear forced vibrations of a suspended cable.
17. A. LUONGO and G. PICCARDO 1998 *Journal of Sound and Vibration* **214**, 915–940. Non-linear galloping of sagged cables in 1:2 internal resonance.
18. M. PAKDEMIRLI, S. A. NAYFEH and A. H. NAYFEH 1995 *Nonlinear Dynamics* **8**, 65–83. Analysis of one-to-one autoparametric resonances in cables-discretization vs. direct treatment.
19. J.-S. WU and C.-C. CHEN 1989 *International Journal for Numerical Methods in Engineering* **28**, 2361–2381. The dynamic analysis of a suspended cable due to a moving load.
20. P. H. WANG, R. F. FUNG and M. J. LEE 1998 *Journal of Sound and Vibration* **209**, 223–249. Finite element analysis of a three-dimensional underwater cable with time-dependent length.
21. C. G. KOH, Y. ZHANG and S. T. QUEK 1999 *ASCE Journal of Engineering Mechanics* **125**, 347–354. Low-tension cable dynamics: numerical and experimental studies.
22. J. A. STRICKLIN and W. E. HAISLER 1977 *Computers and Structures* **7**, 125–136. Formulations and solution procedures for nonlinear structural analysis.
23. F. VENANCIO FILHOR, A. L. G. A. COUTINHO, L. LANDAU, E. C. P. LIMA and N. F. F. EBECKEN 1988 *Computers and Structures* **30**, 979–983. Nonlinear dynamic analysis using the pseudo-force method and the Lanczos algorithm.
24. K.-J. BATHE and S. GRACEWSKI 1981 *Computers and Structures* **13**, 699–707. On nonlinear dynamic analysis using substructuring and mode superposition.
25. B. MOHRAZ, F. E. ELGHADAMSI and C.-J. CHANG 1991 *Earthquake Engineering and Structural Dynamics* **20**, 471–481. An incremental mode-superposition for non-linear dynamic analysis.
26. G. R. DARBRE and J. P. WOLF 1988 *Earthquake Engineering and Structural Dynamics* **16**, 569–581. Criterion of stability and implementation issues of hybrid frequency–time-domain procedure for non-linear dynamic analysis.
27. G. R. DARBRE 1990 *Earthquake Engineering and Structural Dynamics* **19**, 725–738. Seismic analysis of non-linearly base-isolated soil-structure interacting reactor building by way of the hybrid frequency–time-domain procedure.
28. P. HILLMER and G. SCHMID 1988 *Earthquake Engineering and Structural Dynamics* **16**, 789–801. Calculation of foundation uplift effects using a numerical Laplace transform.
29. B. DAVIES and B. MARTIN 1979 *Journal of Computational Physics* **33**, 1–32. Numerical inversion of the Laplace transform: a survey and comparison of methods.
30. P. C. ROBINSON and P. R. MAUL 1991 *Mathematical Engineering in Industry* **3**, 111–131. Some experience with the numerical inversion of the Laplace transforms.

31. D. J. WILCOX 1978 *International Journal of Electrical Engineering Education* **15**, 247–265. Numerical Laplace transform and inversion.
32. H. INOUE, M. KAMIBAYASHI, K. KISHIMOTO, T. SHIBUYA and T. KOIZUMI 1992 *JSME International Journal*, Series I **35**, 319–324. Numerical Laplace transformation and inversion using fast Fourier transform.
33. N. B. KAHLA 1995 *Computers and Structures* **54**, 1197–1211. Dynamics of a single guy cable.
34. H. YAMAGUCHI and Y. FUJINO 1998 *Proceedings of the International Symposium on Advances in Bridge Aerodynamics, Copenhagen, Denmark*, 235–253. Stayed cable dynamics and its vibration control.
35. J. M. KO, Y. Q. NI and J. Y. WANG 2000 *Proceedings of the International Conference on Advanced Problems in Vibration Theory and Applications. Xi'an, China*, 285–291. Tsing Ma suspension bridge: ambient vibration survey campaigns.

APPENDIX A: COEFFICIENTS a_i AND b_i IN EQUATION (9)

$$a_{i1} = -\frac{EA}{\Delta l^2}, \quad a_{i2} = EA\left(\frac{y_i''}{2\Delta l} - \frac{y_i'}{\Delta l^2}\right), \quad a_{i3} = \frac{2EA}{\Delta l^2}, \quad a_{i4} = \frac{2EAy_i'}{\Delta l^2},$$

$$a_{i5} = -\frac{EA}{\Delta l^2}, \quad a_{i6} = -EA\left(\frac{y_i''}{2\Delta l} + \frac{y_i'}{\Delta l^2}\right), \quad b_{i1} = EA\left(\frac{y_i''}{2\Delta l} - \frac{y_i'}{\Delta l^2}\right),$$

$$b_{i2} = \frac{T_i'}{2\Delta l} - \frac{T_i}{\Delta l^2} + EA\left(\frac{y_i'y_i''}{\Delta l} - \frac{(y_i')^2}{\Delta l^2}\right), \quad b_{i3} = \frac{2EAy_i'}{\Delta l^2}, \quad b_{i4} = \frac{2T_i}{\Delta l^2} + \frac{2EA(y_i')^2}{\Delta l^2}.$$

$$b_{i5} = -EA\left(\frac{y_i''}{2\Delta l} + \frac{y_i'}{\Delta l^2}\right), \quad b_{i6} = -\frac{T_i'}{2\Delta l} - \frac{T_i}{\Delta l^2} - EA\left(\frac{y_i'y_i''}{\Delta l} + \frac{(y_i')^2}{\Delta l^2}\right).$$

APPENDIX B: TRANSFORMATION OF EQUATION (14) AS LINEAR REAL ALGEBRAIC EQUATIONS

The Laplace domain parameter p is a complex-valued variable. In the numerical Laplace transform, p is expressed in a discrete form and its value at the lth sample is $p_l = \gamma + \mathrm{j}(2l-1)\pi/T (l = 1, 2, \ldots, N)$. With this expression, the terms in the brackets on the left-hand side of equation (12) can be written as

$$(a_{i3} + mp^2 + c_x p) = a_{i3}^R + \mathrm{j}a_{i3}^I, \qquad (b_{i4} + mp^2 + c_y p) = a_{i4}^R + \mathrm{j}a_{i4}^I, \qquad \text{(B1, B2)}$$

where the subscripts R and I refer to the real and imaginary components respectively. The expressions of a_{i3}^R, a_{i3}^I, a_{i4}^R and a_{i4}^I are given by

$$a_{i3}^R = a_{i3} + m\{\gamma^2 - [(2l-1)\pi/T]^2\} + c_x\gamma, \qquad a_{i3}^I = 2m(2l-1)\gamma\pi/T + c_x(2l-1)\pi/T, \qquad \text{(B3, B4)}$$

$$b_{i4}^R = b_{i4} + m\{\gamma^2 - [(2l-1)\pi/T]^2\} + c_x\gamma, \quad b_{i4}^I = 2m(2l-1)\gamma\pi/T + c_y(2l-1)\pi/T. \qquad \text{(B5, B6)}$$

Similarly, the terms on the right-hand side of equation (12) can be expressed as

$$m[\,pu_i(0) + \dot{u}_i(0)] + c_x u_i(0) + \tilde{P}_{ix}(p) = U_i^R + \mathrm{j}U_i^I, \tag{B7}$$

$$m[\,pv_i(0) + \dot{v}_i(0)] + c_y v_i(0) + \tilde{P}_{iy}(p) + \tilde{f}(x_i, p) = V_i^R + \mathrm{j}V_i^I \tag{B8}$$

in which

$$U_i^R = m[\gamma_i(0) + \dot{u}_i(0)] + c_x u_i(0) + \tilde{P}_{ix}^R(p_l), \tag{B9}$$

$$U_i^I = [m(2l-1)\pi/T]u_i(0) + \tilde{P}_{ix}^I(p_l), \tag{B10}$$

$$V_i^R = m[\gamma v_i(0) + \dot{v}_i(0)] + c_y v_i(0) + \tilde{f}_i^R(p_l) + \tilde{P}_{iy}^R(p_l), \tag{B11}$$

$$V_i^I = [m(2l-1)\pi/T]v_i(0) + \tilde{f}_i^I(p_l) + \tilde{P}_{iy}^I(p_l), \tag{B12}$$

where $\tilde{f}_i^R(p_l), \tilde{f}_i^I(p_l), \tilde{P}_{ix}^R(p_l), \tilde{P}_{ix}^I(p_l), \tilde{P}_{iy}^R(p_l)$ and $\tilde{P}_{iy}^I(p_l)$ are the real parts and imaginary parts of $\tilde{f}(x_i, p)$, $\tilde{P}_{ix}(p)$ and $\tilde{P}_{iy}(p)$ at the lth sample in the Laplace domain.

The transformed displacement components in the Laplace domain, $\tilde{u}_i$, $\tilde{v}_i$ $(i = 1, 2, \ldots, n-1)$, are also complex-valued and can be expressed as

$$\tilde{u}_i = \tilde{u}_i^R + \mathrm{j}\tilde{u}_i^I, \quad \tilde{v}_i = \tilde{v}_i^R + \mathrm{j}\tilde{v}_i^I. \tag{B13}$$

Substituting equations (B1)–(B13) into equation (12) and balancing the real and imaginary parts, respectively, yield

$$a_{i1}\tilde{u}_{i-1}^R + a_{i2}\tilde{v}_{i-1}^R + a_{i3}^R\tilde{u}_i^R - a_{i3}^I\tilde{u}_i^I + a_{i4}\tilde{v}_i^R + a_{i5}\tilde{u}_{i+1}^R + a_{i6}\tilde{v}_{i+1}^R = U_i^R, \tag{B14}$$

$$a_{i1}\tilde{u}_{i-1}^I + a_{i2}\tilde{v}_{i-1}^I + a_{i3}^I\tilde{u}_i^R + a_{i3}^R\tilde{u}_l^I + a_{i4}\tilde{v}_i^I + a_{i5}\tilde{u}_{i+1}^I + a_{i6}\tilde{v}_{i+1}^I = U_i^I, \tag{B15}$$

$$b_{i1}\tilde{u}_{i-1}^R + b_{i2}\tilde{v}_{i-1}^R + b_{i3}\tilde{u}_i^R + b_{i4}^R\tilde{v}_i^R - b_{i4}^I\tilde{v}_i^I + b_{i5}\tilde{u}_{i+1}^R + b_{i6}\tilde{v}_{i+1}^R = V_i^R, \tag{B16}$$

$$b_{i1}\tilde{u}_{i-1}^I + b_{i2}\tilde{v}_{i-1}^I + b_{i3}\tilde{u}_i^I + b_{i4}^I\tilde{v}_i^R + b_{i4}^R\tilde{v}_i^I + b_{i5}\tilde{u}_{i+1}^I + b_{i6}\tilde{v}_{i+1}^I = V_i^I. \tag{B17}$$

Assembly of equations (B14)–(B17) from $i = 1$ to $(n-1)$ results in a system of $4(n-1)$ linear real algebraic equations as

$$\begin{bmatrix} [d_{1,1}] & & & & \\ & \ddots & & & \\ & & [d_{i,i}] & & \\ & & & \ddots & \\ & & & & [d_{n-1,n-1}] \end{bmatrix} \begin{Bmatrix} \{\tilde{u}_1\} \\ \vdots \\ \{\tilde{u}_2\} \\ \vdots \\ \{\tilde{u}_{n-1}\} \end{Bmatrix} = \begin{Bmatrix} \{U_1\} \\ \vdots \\ \{U_2\} \\ \vdots \\ \{U_{n-1}\} \end{Bmatrix} \tag{B18}$$

in which

$$\{\tilde{u}_i\} = \{\tilde{u}_i^R\ \tilde{u}_i^I\ \tilde{v}_i^R\ \tilde{v}_i^I\}^{\mathrm{T}} \quad (i = 1, 2, \ldots, n-1), \tag{B19}$$

$$\{U_i\} = \{U_i^R\ U_i^I\ V_i^R\ V_i^I\}^{\mathrm{T}} \quad (i = 1, 2, \ldots, n-1), \tag{B20}$$

$$[d_{1,1}] = \begin{bmatrix} a_{13}^R & -a_{13}^I & a_{14} & 0 & a_{15} & 0 & a_{16} & 0 \\ b_{13} & 0 & a_{14}^R & -a_{14}^I & b_{15} & 0 & b_{16} & 0 \\ a_{13}^I & a_{13}^R & 0 & a_{14} & 0 & a_{15} & 0 & a_{16} \\ 0 & b_{13} & b_{14}^I & b_{14}^R & 0 & b_{15} & 0 & b_{16} \end{bmatrix}, \tag{B21}$$

$$[d_{i,i}] = \begin{bmatrix} a_{i1} & 0 & a_{i2} & 0 & a_{i3}^R & -a_{i3}^I & a_{i4} & 0 & a_{i5} & 0 & a_{i6} & 0 \\ b_{i1} & 0 & b_{i2} & 0 & b_{i3} & 0 & b_{i4}^R & -b_{i4}^I & b_{i5} & 0 & b_{i6} & 0 \\ 0 & a_{i1} & 0 & a_{i2} & a_{i3}^I & a_{i3}^R & 0 & a_{i4} & 0 & a_{i5} & 0 & a_{i6} \\ 0 & b_{i1} & 0 & b_{i2} & 0 & b_{i3} & b_{i4}^I & b_{i4}^R & 0 & b_{i5} & 0 & b_{i6} \end{bmatrix}, \tag{B22}$$

$$(i = 2, 3, \ldots, n-2),$$

$$[d_{n-1,n-1}] = \begin{bmatrix} a_{n-1,1} & 0 & a_{n-1,2} & 0 & a_{n-1,3}^R & -a_{n-1,3}^I & a_{n-1,4} & 0 \\ b_{n-1,1} & 0 & b_{n-1,2} & 0 & b_{n-1,3} & 0 & b_{n-1,4}^R & -b_{n-1,4}^I \\ 0 & a_{n-1,1} & 0 & a_{n-1,2} & a_{n-1,3}^I & a_{n-1,3}^R & 0 & a_{n-1,4} \\ 0 & b_{n-1,1} & 0 & b_{n-1,2} & 0 & b_{n-1,3} & b_{n-1,4}^I & b_{n-1,4}^R \end{bmatrix}. \tag{B23}$$